

The zebrafish *nodal*-related gene *southpaw* is required for visceral and diencephalic left-right asymmetry

Sarah Long*, Nadira Ahmad and Michael Rebagliati†

Department of Anatomy and Cell Biology, Roy J. and Lucille A. Carver College of Medicine, University of Iowa, Iowa City, IA 52242, USA

*Present address: Neuroscience Graduate Group, University of California, Davis, CA 95616, USA

†Author for correspondence (e-mail: michael-rebagliati@uiowa.edu)

Accepted 12 February 2003

SUMMARY

We have identified and characterized a new zebrafish gene, *southpaw*, that is required for visceral and diencephalic left-right asymmetry. *southpaw* encodes a new member of the nodal-related class of proteins, a subfamily within the transforming growth factor β superfamily of secreted factors. *southpaw* is expressed bilaterally in paraxial mesoderm precursors and then within the left lateral plate mesoderm. At late somite stages, left-sided *southpaw* expression transiently overlaps the left-sided expression domains of other genes that mark the developing heart, such as *lefty2*. We have injected morpholinos to block the translation of the *southpaw* mRNA or to block splicing of the *southpaw* pre-mRNA. These morpholinos cause a severe disruption of early (cardiac jogging) and late (cardiac looping) aspects of cardiac left-right asymmetry. As the left-right asymmetry of the pancreas is also affected,

southpaw appears to regulate left-right asymmetry throughout a large part of the embryo. Consistent with the morphological changes, the left-sided expression domains of downstream genes (*cyclops*, *pitx2*, *lefty1* and *lefty2*) are severely downregulated or abolished within the lateral plate mesoderm of *Southpaw*-deficient embryos. Surprisingly, despite the absence of *southpaw* expression in the brain, we find that early diencephalic left-right asymmetry also requires *Southpaw* activity. These observations lead to a model of how visceral organ and brain left-right asymmetry are coordinated during embryogenesis.

Key words: Zebrafish, *southpaw*, Nodal-related, Left-right, Asymmetry

INTRODUCTION

Nodal-related genes show a conserved pattern of asymmetric expression within the left lateral plate mesoderm (LPM) in mice, chickens and frogs (reviewed by Burdine and Schier, 2000; Capdevila et al., 2000). Genetic and molecular studies implicate this left side nodal domain in the establishment of visceral organ left-right (LR) asymmetry. Nodal functions in this context as part of a conserved LR ‘cassette’, whereby asymmetric nodal signaling induces both conserved downstream antagonists (*Lefty1*, *Lefty2*) and conserved downstream effectors (*Pitx2*) (reviewed by Hamada et al., 2002; Wright, 2001). In the zebrafish, the nodal-related gene *cyclops* (*ndr2* – Zebrafish Information Network) exhibits the same conserved pattern of expression in the left lateral plate as well as additional asymmetric expression within the diencephalon (Rebagliati et al., 1998b; Sampath et al., 1998). However, *cyclops* mutations have, at best, only a small effect on visceral organ LR asymmetry (Bisgrove et al., 2000; Chen et al., 1997; Chin et al., 2000) (M.R., unpublished). This observation is at odds with genetic and molecular studies of other mutations that disrupt nodal signaling in the zebrafish. In particular, the zebrafish *oep* mutation blocks nodal signaling,

and partial loss of zygotic *oep* function severely disrupts both visceral organ and diencephalic LR asymmetry (Gamse et al., 2002; Liang et al., 2000; Yan et al., 1999). Likewise, mutations in the *schmalspur* (*sur*; *foxh1* – Zebrafish Information Network) gene also disrupt LR asymmetry; *sur* encodes another component of the Nodal signaling pathway, the Fast1/FoxH1 protein (Bisgrove et al., 2000; Chen et al., 1997; Pogoda et al., 2000; Sirotkin et al., 2000b).

The lack of congruence between the *cyclops* and *oep/sur* phenotypes raises the issue as to whether the role of asymmetric nodal signaling in LR patterning is conserved in zebrafish vis à vis other vertebrates. One possibility is that nodal signaling is not needed in the left lateral plate in zebrafish, and that the *oep* and *sur* mutations disrupt nodal-dependent signaling from or within the dorsal organizer (reviewed by Burdine and Schier, 2000). Alternatively, the discordance between the *cyclops* and *oep/sur* phenotypes could be reconciled if another nodal-related gene besides *cyclops* were expressed asymmetrically in the lateral plate. The action of this protein, rather than *Cyclops*, would then provide the requisite level of nodal signaling on the left side to establish visceral organ LR asymmetry in the zebrafish. Although mutations in the other zebrafish nodal-related gene, *squint* (*sq*;

ndr1 – Zebrafish Information Network) do disrupt LR asymmetry, *sqt* itself shows no LR asymmetry of expression and it is never expressed within the lateral plate (Feldman et al., 1998; Karlen and Rebagliati, 2001; Rebagliati et al., 1998a). Thus, if Nodal signaling were required within the left lateral plate, this function would have to reflect the action of a new *nodal*-related gene.

To evaluate these possibilities, we have undertaken a degenerate RT-PCR screen for additional zebrafish *nodal*-related genes. We have identified a new zebrafish *nodal*-related gene, which we have named the *southpaw* locus (*spaw*). As implied, *spaw* shows strong left-sided expression within the trunk, as well as bilateral expression within segmental plate (paraxial) mesoderm. Asymmetric expression commences at the 10-12 somite stage, making *spaw* the earliest known molecular marker of LR asymmetry for the zebrafish. We show through loss-of-function experiments with morpholinos that *spaw* is crucially required for the establishment of visceral LR asymmetry, both at the organ level and at the molecular level. Despite the fact that *spaw* is not expressed within the head, we find that *spaw* is also required for the establishment of the earliest aspects of diencephalic LR asymmetry. The anterior limit of asymmetric *spaw* expression lies just rostral to the developing heart. Consequently, our results raise the intriguing possibility that diencephalic LR asymmetry may arise through an Spaw-dependent relay that emanates from the anterior part of the left lateral plate.

In summary, our studies provide strong support for the hypothesis that the role of Nodal signaling in vertebrate LR asymmetry is conserved in the zebrafish. Moreover, these experiments show that the pathways establishing visceral organ and diencephalic LR asymmetry require the same asymmetric cue, the Nodal protein Spaw. Finally, these observations suggest a specific model for how neural and visceral LR asymmetry are coordinated during vertebrate embryogenesis.

MATERIALS AND METHODS

Cloning of *spaw* cDNAs

Degenerate RT-PCR was performed as described (Rebagliati et al., 1998a). A 0.17 kb PCR product was sequenced to confirm homology to *nodal*. Isolation of additional *spaw* (formerly *ndr3*) cDNAs was carried out using PCR screening of a bud to 10-somite stage plasmid cDNA library (Kudoh et al., 2001) and PCR-based amplification of overlapping genomic fragments. A 1.4 kb *spaw* cDNA was subcloned into *pGEMT-Easy* to make *pSpaw-1.4*. The putative initiation codon was identified by comparison of the sequence of the 1.4 kb *spaw* cDNA (GenBank Accession Number AY240027) to overlapping genomic sequence from the Sanger Center's Assembly 6 database.

Construction of *spaw* plasmids

We made an Spaw expression construct, *pCS2+ActHASpaw*, in which the mature region of Spaw is fused to the complete prepro region of Xenopus Activin β A. An HA epitope tag is also present between the proteolytic cleavage site and the N terminus of the mature region. *pCS2+ActHASpaw* was constructed by amplifying the mature region of *spaw* with primers (HASPWF1) and (HASPWR1). After *XhoI/XbaI* digestion, the *spaw* fragment was ligated directionally into *XhoI/XbaI* cut *pCS2+preproAct*. The *XhoI/XbaI pCS2+preproAct* backbone was prepared by digestion of *pCS2+AXnr1* (Piccolo et al., 1999) to remove the *xnr-1* mature region and gel isolation of the

resulting vector/preproactivin/HAtag fragment. *pSpaw(-MATR)* was derived from *pSpaw-1.4* by digesting with *NcoI* and *AfeI* to delete the mature region and then blunting and religating the *vector+preproSpaw* backbone. *pSpaw(-MATR)* was used to generate an *spaw* prepro-region-specific probe.

DNA oligonucleotides

HASPWF1: 5'-TTG-CTCGAGAACCGTGTGGAAAGGATGCG-3'
HASPWR1: 5'-AGTCTAGATCATCAATGACAGCCGCACTC-3'

Morpholino oligonucleotides

Gene Tools' Negative Control MO (NC-MO): 5'-CCTCTTACCTC-AGTTACAATTTATA-3'

Cyclops-MO1: 5'-GCGACTCCGAGCGTGTGCATGATG-3'

Spaw-MO1: 5'-GCACGCTATGACtGGCTGCATTGCG-3'

Spaw-MO2: 5'-TGGTAGAGCTTCAACAGACTCTGCA-3'

Lower case letters: substitutions to reduce MO secondary structure.

The specificity and efficacy of Cyclops-MO1 has been validated previously (Karlen and Rebagliati, 2001). Spaw-MO1 is complementary to a region spanning the putative translation start site (Fig. 1A). For comparison, corresponding sequences of the *cyclops*, *sqt* and *spaw* mRNAs are 5'-CATCATGCACGCGCTCGGAGT-CGCG-3' (initiation codon in bold), 5'-TGACATGTTTTCTGCG-GGCTCCTG-3' and 5'-CGCAATGCAGCCGGTCATAGCGTGC-3', respectively.

Spaw-MO2 overlaps the last exon-intron junction within the *spaw* open reading frame (Fig. 1A). The position of this intron is conserved in many *nodal*-related genes. Corresponding sequences of the *cyclops*, *sqt* and *spaw* pre-mRNAs are 5'-TGCAGAGTTTGCTGA(A/C)AT-ATCATCA-3' (intron in bold), 5'-TGCAGAGTCTTTTGAAGC-TGCACCA-3' and 5'-TGCAGAGTCTGTTGAAGCTCTACCA-3', respectively.

The mismatches between Spaw-MO1/2 and the *cyclops* and *sqt* mRNAs/pre-mRNAs are sufficient to provide specificity. The specificity of Spaw-MO1 and Spaw-MO2 was confirmed by the absence of *cyclops* and *sqt* phenotypes, the absence of dorsal midline defects, and by rescue (see text).

Embryo injections

For production of native Spaw prepro protein, *pSpaw-1.4* was linearized with *NcoI* and transcribed with SP6 polymerase. For production of ActHASpaw, *pCS2+ActHASpaw* was linearized with *NotI* and transcribed with SP6. RNA and DNA injections into two- to 16-cell embryos were carried out as described (Rebagliati et al., 1998a). Morpholinos were diluted into 1xDanieau's and injected at the one- to eight-cell stage into the yolk, just under the blastoderm. Typically, 5-10 ng of a morpholino was injected per embryo in a volume of 2-3 nl.

Whole-mount in situ hybridization analysis and immunohistochemistry

Embryos were fixed in 4% paraformaldehyde. Single probe in situ was carried out using a digoxigenin-labeled antisense RNA probe (Tsang et al., 2000) or with a dinitrophenol-labeled antisense RNA probe as described (Long and Rebagliati, 2002). Two-color (BM Purple and INT RED)/two-probe in situ hybridization was carried out using Dig- and FI-labeled probes (Liang et al., 2000) or, for less abundant transcripts, using Dig- and DNP-labeled probes (Long and Rebagliati, 2002). *pSpaw-1.4* was used to make the *spaw* probe. We used a full-length *pitx2c* cDNA to make a *pitx2* probe that hybridizes to all the *pitx2* mRNA isoforms (Essner et al., 2000). Immunohistochemistry with the myosin MF20 antibody was carried out described (Rebagliati et al., 1998a) but using cobalt-enhanced DAB.

Mutant analysis

The following alleles were used: *sqt*^{c235}, *boz*^{m168}, *cyc*^{b16}, *ntl*^{b160} and *flh*ⁿ¹. *boz*^{m168} homozygotes were identified by the presence of severe

notochord defects (corresponding to classes III-V of the *boz* phenotypic series) (Fekany et al., 1999).

Scoring organ LR asymmetry

Cardiac jogging was assayed visually or by whole-mount in situ hybridization with an *nkx2.5* probe. Heart looping was assayed visually or by staining with the myosin heavy chain antibody MF20. Pancreatic LR asymmetry was determined at 48-72 hours post-fertilization using a zebrafish *preproinsulin* probe (Milewski et al., 1998).

RESULTS

Spaw encodes a member of the Xnr1 subclass of the nodal-related protein family

Spaw is a new member of the *nodal* subfamily of the TGF β superfamily (Fig. 1A), as judged by the following criteria:

(1) In terms of overall amino acid identity, the Spaw protein is more closely related to Nodal-class proteins than to other subfamilies within the TGF β superfamily.

(2) The Spaw protein sequence contains the two amino acid motifs, NAYRCEG and PTNHAY, which unequivocally distinguish the *nodal*-related subfamily from other subfamilies.

(3) In at least some *nodal*-related genes, there is an intron that interrupts the open reading frame encoding the mature ligand domain; this intron is present within the *spaw* locus and interrupts the open reading frame at the same relative position as seen in the *nodal*, *cyclops* and *sqt* genes (Zhou et al., 1993) (M.R., unpublished).

One can draw an additional distinction by looking at the spacing of the seven conserved cysteines within the mature ligand domain of the Spaw polypeptide. Nodal-related proteins fall into two subclasses based on two distinct patterns of cysteine residues (Jones et al., 1995). One subclass includes the mouse *nodal* and zebrafish *Cyclops* proteins; the other includes the *Xenopus* Nodal-related 1 (Xnr1) and zebrafish *Sqt* proteins. The Spaw protein contains the split-cysteine arrangement that is characteristic of the Xnr1 subtype (Fig. 1A). Overall, Spaw shares more amino acid identity with *Xenopus* Nodal-related 1 than with zebrafish *Cyclops* (Fig. 1B); this is also consistent with its classification within the Xnr1 subgroup.

Developmental expression profile of *spaw*

We determined the developmental profile of *spaw* expression using whole-mount RNA in situ hybridization. No *spaw* expression is detected prior to somitogenesis. The earliest detectable *spaw* expression consists of two bilateral domains flanking the tailbud; these domains first appear at the four- to six-somite stage and persist into later stages of somitogenesis (Fig. 2A, inset in Fig. 2M). By 24 hours post-fertilization, expression in these areas is strongly downregulated but trace amounts of *spaw* expression are still visible (not shown). To determine within which anlagen these bilateral domains lie, we performed double probe in situ hybridization with a *spaw* probe and a *spadetail* (*spt*) or *no tail* (*ntl*) probe. *spaw* transcripts overlap with *spt* expression within adaxial cells and presomitic mesoderm but are excluded from the *ntl*-positive notochord (Fig. 2B-D). There may be overlap between *spt*, *ntl* and *spaw* in the area where presomitic mesoderm merges into the tailbud. These results indicate that, at least during early

somitogenesis, the bilateral *spaw* domains lie within the regions containing paraxial mesoderm precursors (Griffin et al., 1998; Schulte-Merker et al., 1994).

Asymmetric *spaw* expression in the left lateral plate mesoderm is first detected in about 75% of the embryos at the 10-12 somite stage, in a posterior domain near the tailbud, and in all of the embryos shortly thereafter (Fig. 2E). *spaw* expression in the left lateral plate precedes asymmetric *lefty2*, *cyclops* or *pitx2* expression: left-sided expression of these genes is first detected between the 17- and 22-somite stages, depending on the particular gene (Bisgrove et al., 1999; Essner et al., 2000; Rebagliati et al., 1998b; Sampath et al., 1998). Thus, *spaw* is currently the earliest molecular marker of LR asymmetry in the zebrafish. Asymmetric *spaw* expression then spreads in a posterior-to-anterior (PA) fashion (Fig. 2F,J); this progression is reminiscent of the PA extension of the left-sided domain of the *xnr1* gene (Lowe et al., 1996). Subsequently, left-sided *spaw* diminishes in a caudal to rostral progression, while expanding laterally at the same time (Fig. 2K,L). Left-sided *spaw* expression is then downregulated rapidly (Fig. 2M).

As the protein One-eyed Pinhead (Oep) is required for signaling by Nodal-related proteins, *oep* and *spaw* expression would be expected to overlap or to be adjacent (Gritsman et al., 1999). In situ hybridization with *oep* and *spaw* probes show that, from the 10- to 17-somite stages, *oep* and *spaw* expression coincide temporally and either overlap in the lateral plate or are in close proximity (Fig. 2F,G). However, unlike *oep*, *spaw* is not expressed in the head (Fig. 2H,I).

Two-color in situ hybridization was carried out to compare the expression domains of *spaw* with those of *lefty2* and *pitx2*: two asymmetrically expressed genes that are known to be Nodal dependent in other organisms. To improve sensitivity, we have modified the standard protocol by replacing the fluorescein label with a different hapten: dinitrophenol (Long and Rebagliati, 2002). The observed in situ patterns are consistent with the interpretation that left-sided *spaw* precedes (Fig. 3A) and then transiently overlaps the left-sided *lefty2* and *pitx2* expression domains in the trunk (Fig. 3B-E for *lefty2*; *pitx2* data not shown). The anteroposterior (AP) boundary of the left-sided *spaw* domain terminates just rostral to that of *lefty2* (Fig. 3D); *lefty2* expression marks the heart field at these stages. Our results echo previous studies comparing *cyclops*, *lefty1/2* and *pitx2*; these studies also found overlapping and exclusive domains for these four genes within the heart field (Bisgrove et al., 2000). *pitx2*, *cyclops* and *lefty1* also exhibit overlapping left-sided asymmetry within the epiphyseal region of the diencephalon. However, *spaw* is not expressed in the diencephalon (Fig. 2H; Fig. 3F; data not shown).

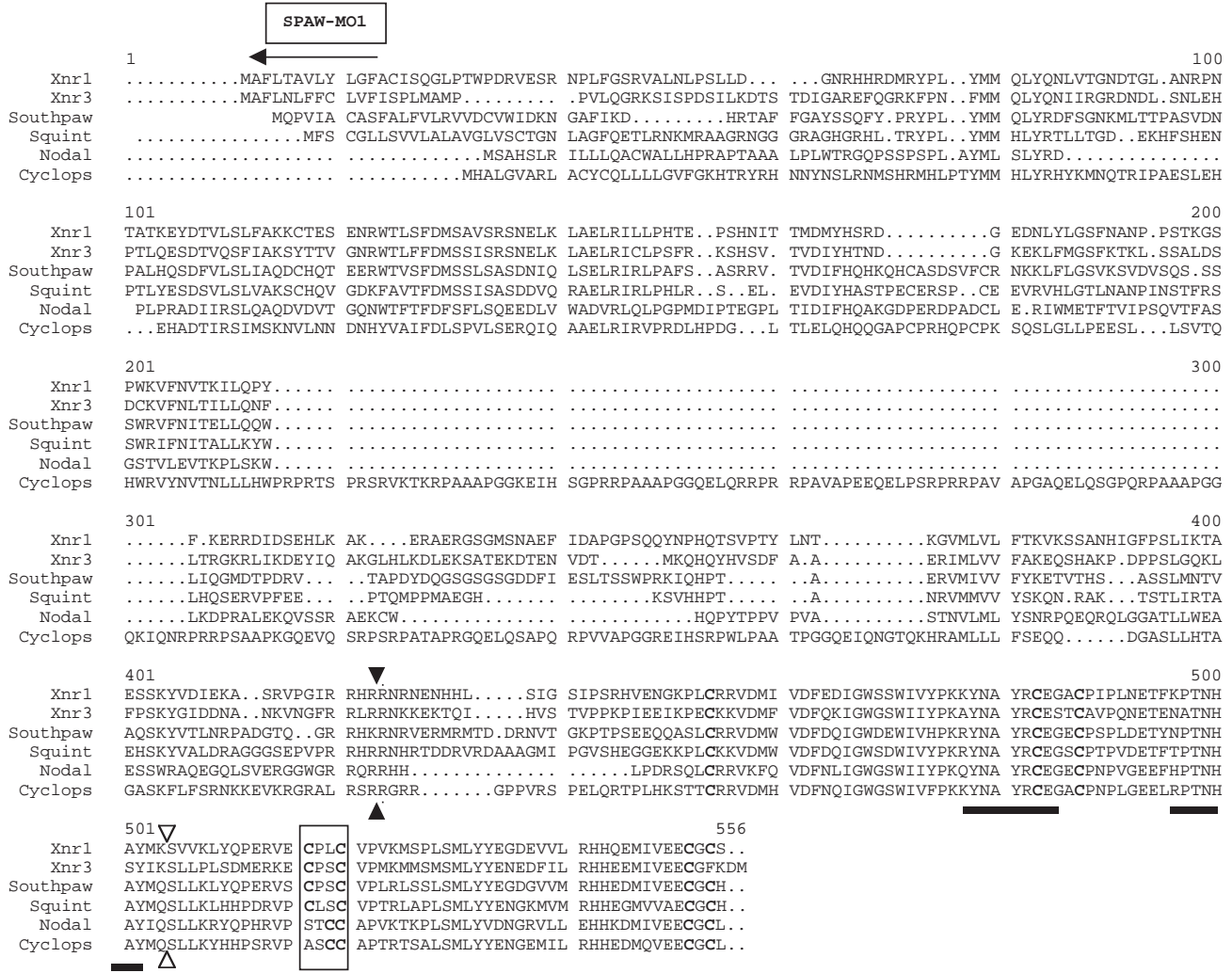
Effects of dorsal midline mutations on *spaw* expression

Proper development of the dorsal midline is needed for the establishment and maintenance of the LR axis. This reflects two roles: (1) a role for the organizer in propagating early LR asymmetry cues to the lateral plate, and (2) a role for dorsal structures such as the notochord and floor plate as midline barriers (Danos and Yost, 1996) (reviewed by Burdine and Schier, 2000; Capdevila et al., 2000). Zebrafish midline mutations that disrupt LR asymmetry generally lead to either the abrogation or to the bilateral expression of

asymmetrically expressed genes, such as *cyclops*, *pitx2*, *lefty1* and *lefty2* (Bisgrove et al., 2000; Concha et al., 2000; Liang et al., 2000; Yan et al., 1999). To determine if the asymmetric expression of *spaw* was also dependent on the correct development of the dorsal midline, we analyzed five mutations (*cyc^{b16}/hhex*, *ntl^{b160}*, *flhⁿ¹*, *sqt^{cz35}* and *boz^{m168}*) that

have been implicated in development of the shield (dorsal organizer) or its derivatives (the prechordal mesoderm, notochord and forerunner cells). *cyc^{b16}/hhex* is a deletion that removes both *cyclops* and *hhex*, a homeobox gene expressed in the yolk syncytial layer (YSL), endoderm and other tissues (Ho et al., 1999; Liao et al., 2000). The effect of the *cyc^{b16}*

A



B

% aa identity	Sqt prepro	Cyc prepro	Xnr1 prepro	Sqt mature	Cyc mature	Xnr1 mature
Spaw prepro	29%	17%	24%			
Spaw mature				61%	56%	63%

Fig. 1. (A) Alignment of Spaw and other Nodal-related proteins. Black arrowheads indicate putative cleavage sites between the prepro and mature ligand domains (RXRR). Open arrowheads indicate position of a conserved intron. Arrows indicate peptide stretches where the corresponding nucleotide sequences are complementary to the morpholinos Spaw-MO1 and Spaw-MO2. Heavy underlining indicates nodal-specific motifs (NAYRCEG and PTNHAY). The boxed region highlights the split cysteine pattern (CXXC) that differentiates the Xnr1/Sqt subclass and Nodal/Cyclops subclass (XXCC). (B) Amino acid identity (%) between the *spaw* prepro domain or mature domain and the corresponding domains of Sqt, Cyclops and Xnr1.

deletion on LR asymmetry reflects the loss of *hhex* function in the YSL rather than the lack of *cyclops* (Wallace et al., 2001).

In terms of LR asymmetry, the main effect of the *ntl* and *floating head* (*flh*) mutations is to cause bilateral expression of normally asymmetric markers (*lefty2*, *pitx2*) within the diencephalon and lateral plate [however, note that the primary effect of *flh* on *lefty2* in the LPM was reported by one group to be loss of *lefty2* expression (Chin et al., 2000)]. Consistent with these reports, we observed mainly bilateral expression of *spaw* in the lateral plate of *ntl^{b160}* or *flhⁿ¹* homozygotes (Table 1, Fig. 4A,B). The *boz^{m168}* and *cyc^{b16}/hhex* alleles were reported to abolish LPM expression of *lefty1*, *lefty2* and *pitx2* (Chin et al., 2000). By contrast, we observed that the primary effect of *boz^{m168}* and *cyc^{b16}/hhex* was to cause bilateral expression of *spaw* within the LPM (Table 1). We do not know the reason for this difference, but the known variability of the *boz* phenotype could be a contributing factor (Fekany et al., 1999). *sqt^{cz35}* causes bilateral expression of *pitx2*, *lefty2* and *cyclops* in the diencephalon, but effects on visceral asymmetry have not been reported (Liang et al., 2000). We find that the predominant effect of this mutation is bilateral expression of *spaw* within the lateral plate (Table 1, Fig. 4D). Right-sided (reversed) expression of *spaw* was observed only at a low frequency, most often in *boz^{m168}* and *cyc^{b16}/hhex* homozygotes (Table 1, Fig. 4E). Overall, our results indicate that correct left-sided regulation of *spaw* also depends on the normal development of the dorsal midline.

The *cyc^{b16}/hhex*, *flhⁿ¹*, *sqt^{cz35}* and *boz^{m168}* mutations did not have any effect on the bilateral zones of *spaw* expression that flank the tailbud. However, in *ntl^{b160}* homozygotes, these bilateral domains are lost (Fig. 4B), indicating that normal *spaw* expression in the

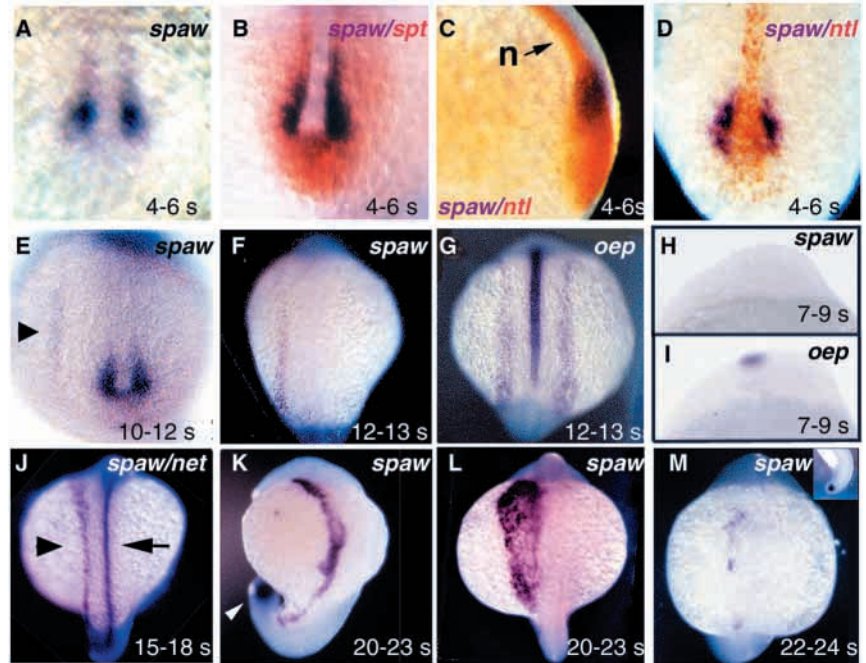


Fig. 2. *Spaw* expression. (A-D) Four to six somite stage. (A) Dig-*spaw* probe, dorsal close-up of tailbud. (B-D) Two-color in situ hybridization: *spaw* probe and a *spadetail* or *ntl* probe. (B) Dig-*spaw* (purple) + Fl-*spt* (red), dorsal view of tailbud. (C) Dig-*spaw* (purple) + Fl-*ntl* (red), lateral view of tailbud. n, prospective notochord. (D) Dig-*spaw* (purple) + Fl-*ntl* (red), dorsal view of tailbud. (E) Ten to 12 somite stage. Dig-*spaw*, dorsal view, onset of asymmetric left-sided expression (arrowhead). (F,G) Twelve to 13 somites, dorsal views, comparing *spaw* (F) and *one-eyed pinhead* (G) expression. Anterior is towards the top. (H,I) Seven to nine somite stage, lateral view, close-up of heads. Anterior is towards the right. (H) Dig-*spaw* probe. (I) Dig-*oep* probe. (J-M) Dorsal views, anterior towards the top. (J) Fifteen to 18 somites, DNP-*spaw* plus a DNP-*netrin* probe. Arrowhead indicates left-sided *spaw* domain. Arrow indicates central stripe of *netrin* in floor plate. (K,L) Twenty to 23 somite stage. (K) Dig-*spaw* (purple) showing left-sided *spaw* domain along most of the length of the embryo. White arrow indicates bilateral *spaw* flanking tailbud. (L) Left-sided *spaw* domain has expanded laterally and is fading posteriorly. (M) Twenty-two to 24 somite stage; Dig-*spaw* probe (inset provides a lateral view of the tailbud).

paraxial mesoderm also requires *ntl* function. At a low frequency, we also saw ectopic *spaw* expression in the notochord of wild-type siblings from *ntl* incrosses (Fig. 4C).

Fig. 3. Comparison of *spaw* with *lefty2* and *pitx2*. (A,C,D) Dig-*spaw* (purple) + DNP-*lefty2* (red) probes. Dorsal close-up; A is at a lower magnification than C and D; *lefty2* marks the heart field. (A,C,D) The patterns seen in embryos from a pool of 20-23 somite embryos. (A) *spaw* is expressed in this embryo but *lefty2* is not. The converse pattern (*lefty2*⁺, *spaw*⁻) was never seen. (B) Dig-*spaw* probe alone, 20-23 somite stage. Dorsal close-up near heart field. Comparison of B (*spaw* probe) with C (*spaw* + *lefty2* probes) emphasizes the extensive overlap between the left-sided *spaw* and *lefty2* expression domains in C. (D) Asymmetric *spaw* and *lefty2* zones are present as largely non-overlapping domains. (E) Dorsal close-up. DNP-*lefty2* probe (red) only, 20-23 somite embryo. (F) Twenty to 23 somite embryo. Dig-*spaw* (purple) + DNP-*pitx2* (red) probes. Lateral view, anterior towards the left, comparing the anterior border of *spaw* (black arrowhead) in the lateral plate with the anterior position of left-sided *pitx2* (arrow) in the diencephalon.

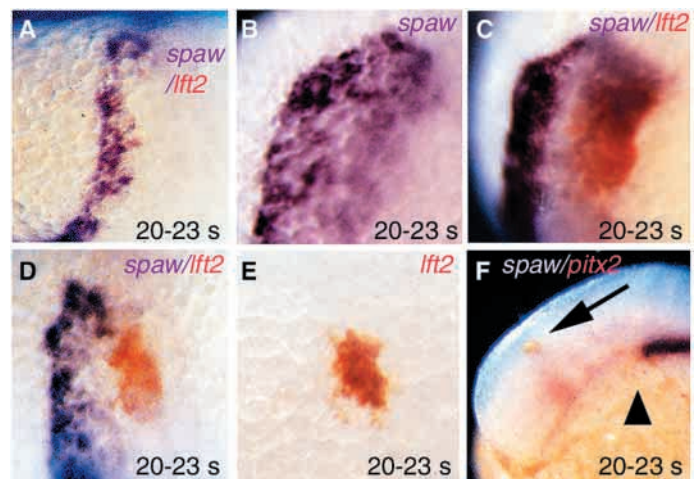
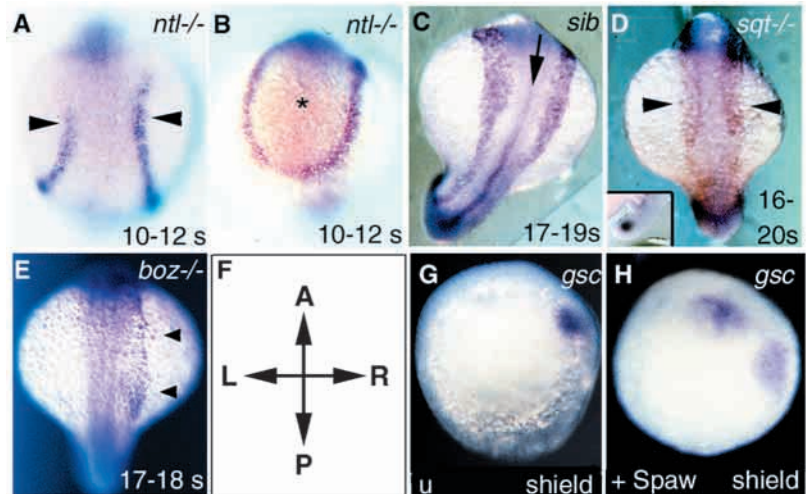


Fig. 4. *Spaw* expression in midline mutants.

(A-E) Dorsal views, anterior is towards the top. Dig-*spaw* probe. (F) Coordinate axes: A, anterior; P, posterior; L, left; R, right. (A,B) Ten to 12 somite stage, *ntl^{b160}/ntl^{b160}* (abbreviated *ntl^{-/-}* in figure) Asterisk indicates tailbud; arrowheads indicate left and right lateral plate. (C) Seventeen to 19 somites. Wild-type sibling (*sib*) from a *ntl^{b160}/+* incross. Arrow indicates ectopic *spaw*. (D) Sixteen to 20 somite embryo, *sqt^{cz35}/sqt^{cz35}* (abbreviated *sqt^{-/-}* in figure) Arrowheads indicate bilateral *spaw* expression in lateral plate. Inset shows lateral view of tailbud. (E) Seventeen to 18 somites, *boz^{m168}/boz^{m168}*. Arrowhead indicates right-sided *spaw* domain. (G,H) Shield stage, looking down on blastoderm, dorsal towards the right, Dig-*gooseoid* probe. (G) Uninjected control. (H) Injected with 25 pg *pCS2+ActHASpaw* plasmid.



Functional analysis of the *spaw* locus: overexpression studies

In order to determine the inductive properties of Spaw, we constructed a chimeric expression vector (*pCS2+ActHASpaw*) in which an HA-epitope tagged version of the Spaw mature domain is fused to the prepro region of *Xenopus* Activin β A. Endogenous *spaw* transcripts can be distinguished from the chimeric transcripts by using a probe specific for the *spaw* prepro-region sequences. Injection experiments with *ActHASpaw* mRNA or *pCS2+ActHASpaw* DNA show that the mature Spaw protein has similar inductive properties to Sqt. Like Sqt, Spaw can induce ectopic *gooseoid* and *cyclops* expression in shield stage embryos, i.e. Spaw has dorsalizing activity (Fig. 4G,H). We also tested a synthetic *spaw* mRNA transcript encoding the native Spaw precursor protein. This showed a qualitatively similar, albeit much weaker dorsalizing activity (data not shown). The lower activity may reflect the absence of some native 5' and 3' UTR sequences but other explanations have not been ruled out. Overexpression of Spaw also disrupts LR asymmetry, as shown by randomization of cardiac LR asymmetry and induction of bilateral expression of endogenous *spaw* transcripts (data not shown). However, dorsalizing mutations are known to disrupt LR asymmetry

(Chen et al., 1997). Thus, the effects of Spaw overexpression on LR asymmetry probably reflect the fact that early zygotic mis-expression of Spaw dorsalizes the embryo.

Functional analysis of the *spaw* locus: morpholino-mediated inhibition of Spaw activity

To block Spaw activity, we designed two *spaw* antisense morpholino oligonucleotides (Fig. 1A). Spaw-MO1 is complementary to sequences near the putative start codon of the *spaw* open reading frame. Spaw-MO2 is complementary to the splice acceptor site for the last exon. The last two exons encode the mature ligand domain of the Spaw polypeptide. The use of two morpholinos targeted to different *spaw* sequences provides a stringent control for specificity. In addition, we also compared the effects of the *spaw* morpholinos to the effects of a *cyclops* morpholino (Cyclops-MO1) and/or a standard negative control morpholino (NC-MO) that is not complementary to *spaw* sequences.

Given that disruptions of the dorsal midline can perturb LR asymmetry, it was important to verify that Spaw-MOs do not disrupt the normal development of dorsal structures. By both molecular and morphological criteria, dorsal midline development proceeded normally in Spaw-MO1-injected embryos (Fig. 5A-D; see Fig. 7B). There was no cyclopia (Fig. 5D) or floor plate defect (see Fig. 7B), which suggests that prechordal mesoderm and ventral CNS development are normal. These observations also indicate that the *spaw* morpholino did not inhibit the other two *nodal*-related genes, *cyclops* and *sqt*, as such ventral CNS defects are a hallmark of the *cyclops* and *sqt* phenotypes. The somites and the notochord were also grossly normal, comparing Spaw-MO1 and uninjected embryos (Fig. 5A-D). Likewise, Spaw-MO2-injected embryos did not exhibit any cyclopia or axial mesodermal defects, again showing that neither *cyclops/sqt* function nor midline development was affected significantly (data not shown). To verify these conclusions using molecular criteria, we examined the expression of five dorsal midline markers (*gooseoid*, *sqt*, *ntl*, *netrin* and *lefty1*) at various times during gastrulation (60-70% epiboly) or somitogenesis (1-3 somites, 6-7 somites, 17-18 somites). In all cases, gene expression was similar between uninjected and Spaw-MO1-injected embryos (Fig. 5E, Fig. 6, Fig. 7B,C; data not shown).

Table 1. Effect of midline mutations on *southpaw* expression

Genotype	Lateral plate expression (%)				
	<i>n</i>	L	R	B	A
<i>boz m168/boz m168</i>	26	27	12	61	0
Wild-type sibs	95	93	1	6	0
<i>cyc b16/cyc b16</i>	14	14	14	57	14
Wild-type sibs	58	90	3	3	3
<i>flh n1/flh n1</i>	18	33	6	50	11
Wild-type sibs	65	94	0	6	0
<i>ntl b160/ntl b160</i>	13	0	0	100	0
Wild-type sibs	66	97	0	3	0
<i>sqt cz35/sqt cz35</i>	27	26	7	63	4
Wild-type sibs	143	81	6	11	2

n, number of embryos; L, left; R, right; B, bilateral; A, absent. Analyzed at 15-19 somites.

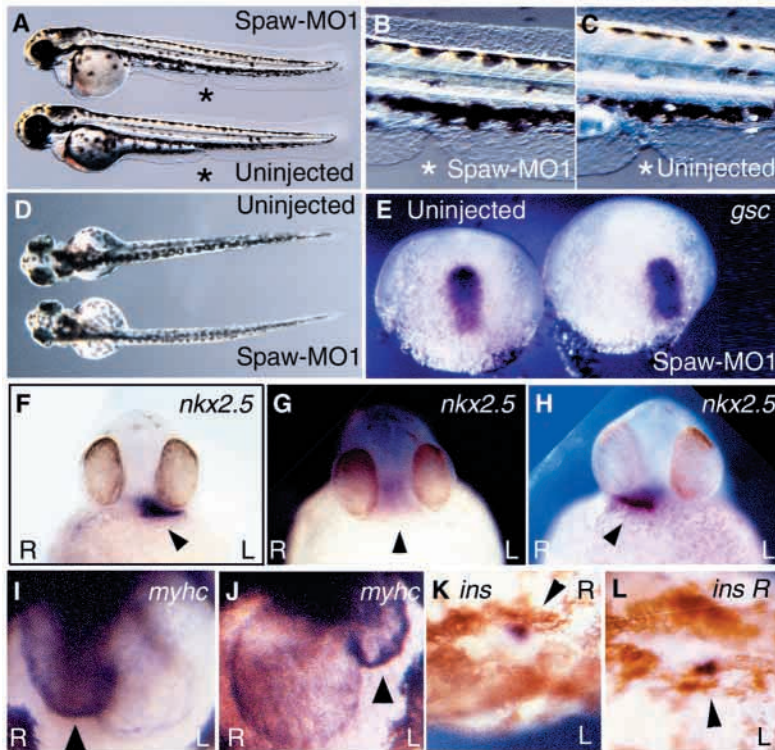


Fig. 5. Morphological effects of *spaw* knockdown. (A-D) Uninjected and Spaw-MO1-injected embryos (10 ng), 55-60 hours post-fertilization embryos.

(A) Lateral view, anterior towards the left. Asterisks indicate posterior end of yolk tube extension. (B,C) Higher magnifications of embryos in A, focusing on somites and notochord. (D) Dorsal view, anterior towards the left. (E) Sixty to 70% epiboly, Dig-*gsc* probe, dorsal view. Uninjected embryo (left); embryo injected with 10 ng Spaw-MO1 (right). (F-H) Ventral anterior view of 30 hours post-fertilization embryos injected with 6 ng Spaw-MO1. Dig-*nkx2.5* probe shows the heart tube (arrowheads). Hearts exhibit left jog (F), no jog (G) or right jog (H). (I,J) MF20 myosin antibody staining highlighting normal D-looping (I) and reversed L-looping (J) of the heart in two embryos injected with 10 ng each of Spaw-MO1. Ventral views, 60 hours post-fertilization. The ventricle (arrowhead) stains more intensely. (K,L) Dorsal view of 48 hours post-fertilization embryos (anterior towards the left), Dig-*preproinsulin* probe, right (K) and left (L) displacements of the pancreas (arrowheads) from the midline. R, right side; L, left side.

There were no obvious changes in Spaw-MO2-injected embryos, either; this was checked using two midline markers that are sensitive to reductions in Sqt or Cyclops activity [*gooseoid* (shield stage) and *netrin* (16-20 somites); data not shown]. As these experiments suggested that LR phenotypes would be interpretable in Spaw-deficient embryos, we proceeded to analyze the effect of these morpholinos on LR asymmetry.

Cardiac jogging and looping are *spaw*-dependent events

For zebrafish embryos, the earliest visible signs of LR asymmetry are changes in heart tube position and morphology (Chen et al., 1997). The relatively straight heart tube first shifts or 'jogs' to the left of the dorsal midline; this leftward jogging is most evident from about 26-30 hours post-fertilization (Fig. 5F). The heart tube then acquires a rightward or D-loop and assumes its final AP orientation from 30-60 hours post-

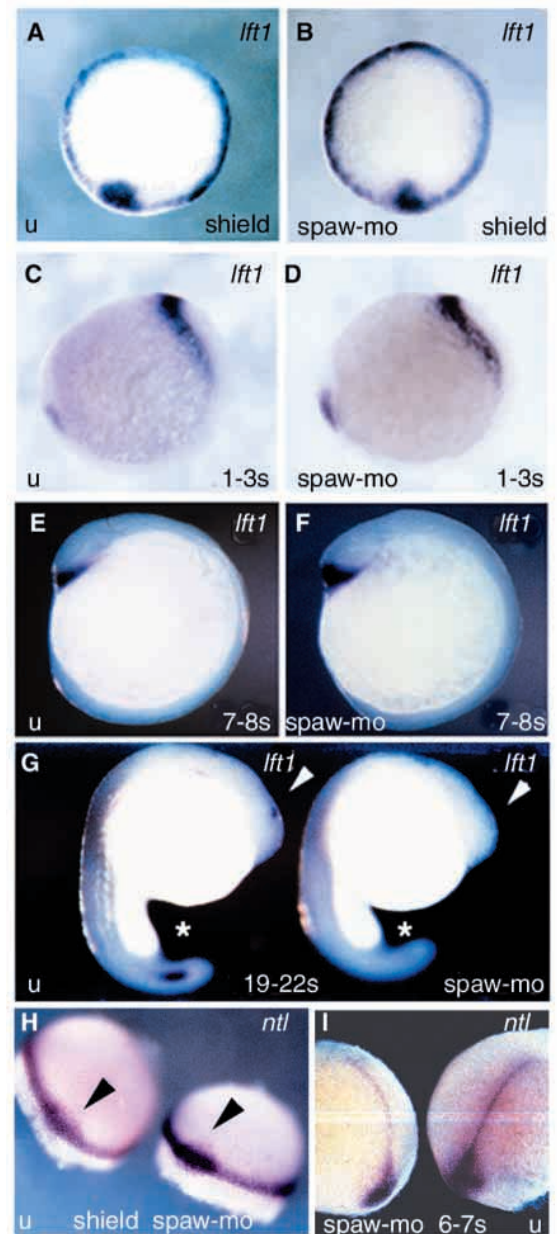


Fig. 6. The effects of *spaw* inhibition on midline development are restricted to effects on late *lefty1* expression. (A-G) Comparison of *lefty1* expression in uninjected (u) and Spaw-MO1-injected (10 ng) embryos at various stages. Dig-*lefty1* probe. (A,B) Shield stage. (C,D) One to 3 somite stage. (E,F) Seven to 8 somite stage. (G) nineteen to 22 somite stage. (A,B) View onto blastoderm, dorsal is downwards. (C-F) Lateral views, anterior towards the top. (G) Lateral views, anterior towards the upper right. Arrowheads indicate presence (left) or absence (right) of asymmetric *lefty1* expression in diencephalon. Asterisks indicate presence (left) or absence (right) of *lefty1* in posterior notochord. (H,I) Comparison of *ntl* expression in uninjected (u; left in H, right in I) and Spaw-MO1-injected (10 ng; right in H, left in I) embryos at shield and 6-7 somite stages. Dig-*ntl* probe. (H) Arrowheads indicate *ntl* expression in dorsal shield and forerunner cells. (I) Views of dorsal midline, anterior is towards top.

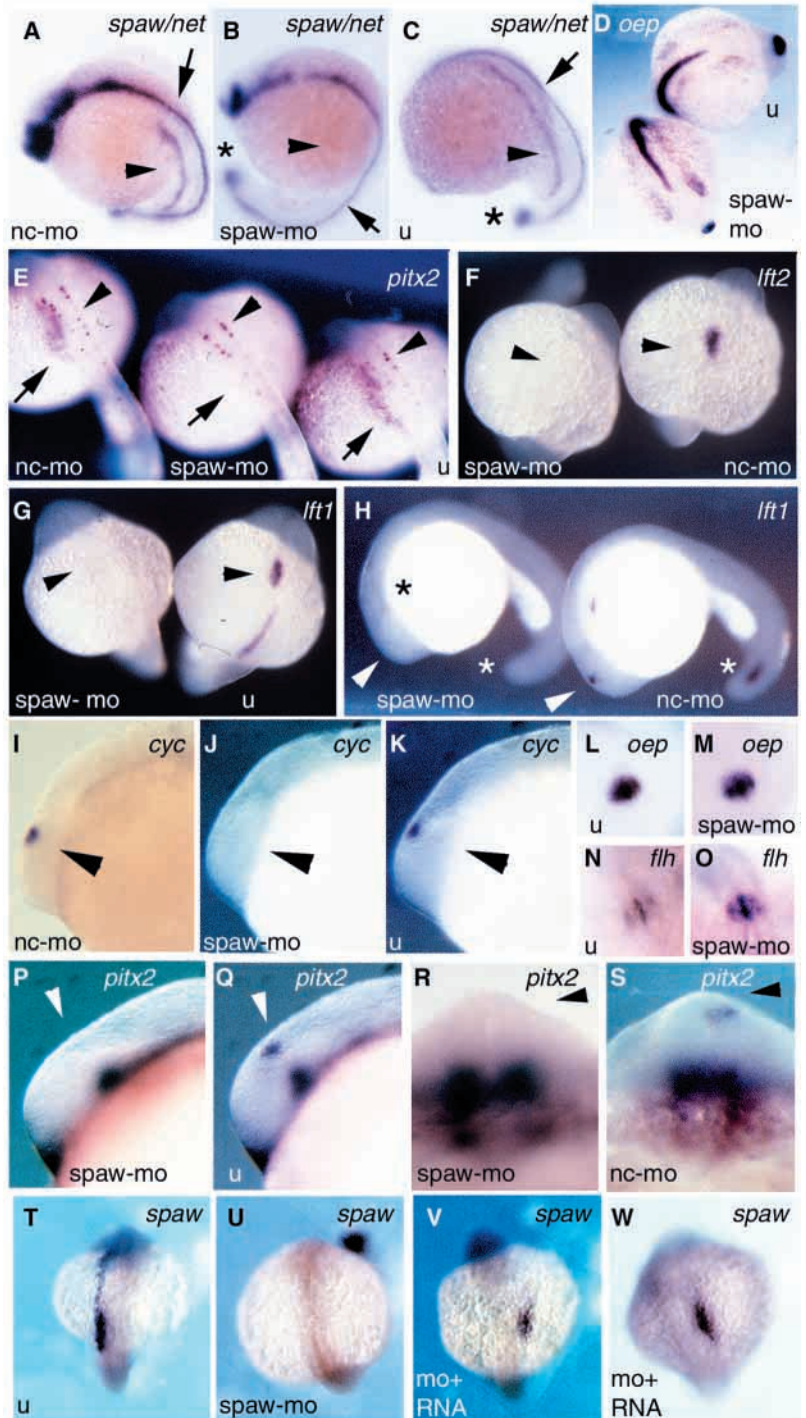
fertilization (Fig. 5I). Zebrafish LR asymmetry mutants can be categorized by whether they disrupt the normal linkage

between cardiac jogging and cardiac looping (Chin et al., 2000). With some zebrafish LR mutations (e.g. *spt^{b104}*, *din^{tt250}* and *cyc^{b16/hhex}*) one sees correlated reversals in both jogging and looping, e.g. embryos with reversed jogs (right jogs) tend to form hearts with reversed looping (L-looping). Other zebrafish LR mutations (e.g. *mom^{th211}*, *boz^{m168}*, *flhⁿ¹* and *ntl^{b160}*) uncouple jogging and looping. This dichotomy has been interpreted as evidence that heart placement (relative to

the midline) and heart looping are established by two separable mechanisms: early LR asymmetry cues within the lateral plate mesoderm would bias heart placement (jogging), and a later process would somehow translate this initial heart position into a heart looping chirality. We examined Spaw-MO-injected embryos to determine whether decreases in Spaw affected cardiac jogging and looping polarity, as well as the coupling between these two events.

Fig. 7. *spaw* regulates asymmetric gene expression.

(A-C) Seventeen to 18 somite stage, DNP-*netrin* + DNP-*spaw* probes. Arrows indicate *netrin* (*net*) in the CNS. Arrowheads indicate the presence (A,C) or absence (B) of *spaw* in the left lateral plate. Asterisk indicates *spaw* expression in the tailbud. (A) 10 ng NC-MO; (B) 10 ng Spaw-MO1; (C) uninjected (u). (D) Twelve to 14 somite stage, Dig-*oep* probe. (Top) Uninjected; (Bottom) injected with 14 ng Spaw-MO1. (E) Twenty-two to 24 somite stage; Dig-*pitx2* probe, dorsal view of embryos injected with 10 ng NC-MO (left), 10 ng of Spaw-MO1 (middle) or not injected (right). Black arrows indicate position of left-sided *pitx2c* near gut. Black arrowheads indicate bilateral *pitx2a/2c* in putative Rohon-Beard neurons. (F) Twenty to 22 somite stage; Dig-*lefty2* probe; dorsal view with anterior towards the top. (Left) 10 ng Spaw-MO1 treated; (Right) 10 ng NC-MO treated. Arrowheads indicate presence (right) or absence (left) of left-sided *lefty2* domain. (G) Nineteen to 22 somite stage; Dig-*lefty1* probe; dorsal view with anterior towards the top. (Right) Uninjected; (Left) injected with 10 ng Spaw-MO1. Arrowheads indicate presence (right) or absence (left) of left-sided *lefty1* domain in heart. (H) Nineteen to 22 somites, lateral view, anterior towards the left. Dig-*lefty1* probe. Embryos injected with 10 ng of Spaw-MO1 (left) or of NC-MO (right). Asterisks indicate site of *lefty1* expression domain in posterior notochord. Arrowheads indicate location of *lefty1* domain on left side of dorsal diencephalon. (I-K) Eighteen to 22 somites; DNP-*cyclops* probe; lateral view of head, anterior towards the left. (I) Embryo injected with 10 ng of NC-MO. (J) Embryo injected with 10 ng Spaw-MO1. (K) Uninjected embryo. Arrowheads indicate expression (I,K) or absence (J) of *cyclops* in the left part of the dorsal diencephalon. (L,M) Twelve to 14 somites, anterior towards the bottom; Dig-*oep* probe, dorsal view, focusing on the epiphysis. (L) Uninjected embryo. (M) Embryo injected with 14 ng Spaw-MO1. (N,O) Nineteen to 23 somites; Dig-*flh* probe, dorsal view, focusing on epiphysis. (N) Uninjected embryo. (O) Embryo injected with 10 ng Spaw-MO2. (P,Q) Twenty-one to 23 somite stage; DNP-*pitx2* probe; lateral views (left side), anterior towards the left. Arrowheads indicate region of the dorsal diencephalon where *pitx2c* mRNA is normally restricted to the left side. (P) Embryo injected with 10 ng of Spaw-MO1. (Q) Uninjected embryo. (R,S) Twenty-one to 23 somite stage, DNP-*pitx2* probe, frontal view. Arrowheads indicate region of the dorsal diencephalon where *pitx2c* mRNA is normally restricted to the left side. (R) Embryo injected with 10 ng of Spaw-MO1. (S) Embryo injected with 10 ng of NC-MO. (T-W) Sixteen to 18 somite stage; anterior is towards the top, dorsal view. DNP-*spaw(-MATR)* probe is specific for endogenous *spaw* transcripts. (T) Uninjected embryo. (U) Embryo injected with 9 ng of Spaw-MO1. (V,W) Two examples of 'spaw-reversed' embryos, achieved by co-injection of 9 ng Spaw-MO1 and 40 pg *ActHASpaw* RNA.



In Spaw-MO-injected embryos, the LR asymmetry of cardiac jogging was severely disrupted. There was a large increase in the frequency of embryos with either right (reversed) or no jogs, with the latter being the more prevalent effect (Table 2A; Fig. 5G,H). These effects were seen with Spaw-MO1 and Spaw-MO2 but were not seen with doses of a Cyclops-MO that are sufficient to phenocopy the *cyclops* mutation or with comparable doses of an unrelated morpholino (Table 2A).

To determine whether Spaw knockdown uncoupled jogging and looping polarity, we segregated Spaw-MO1-injected embryos into cohorts based on their jogging phenotype, and scored each cohort for cardiac looping phenotypes at 48 and 60-65 hours post-fertilization. This analysis showed that the Spaw knockdown phenotype resembles the ‘uncoupling’ class of LR mutants: Spaw-MO1 disrupts the LR bias of both jogging and looping and unlinks the two events (Table 2B, Fig. 5I,J). D-looping is favored slightly in Spaw-MO-injected embryos, but this is also true for uncoupling mutants. There was one significant difference between Spaw-knockdown embryos and the uncoupling class of LR mutants. In Spaw-MO-injected embryos, unlooped hearts occurred with a higher frequency than L-looped hearts, irrespective of jogging polarity. By contrast, for *mom^{th211}*, *boz^{m168}*, *flhⁿ¹* and *ntl^{b160}* homozygotes, L-looped hearts were reported to be more common than hearts with no looping (Chin et al., 2000). In summary, these results show that *spaw* is crucial for both early and late aspects of cardiac LR asymmetry and that loss of *spaw* function is similar, though not identical, to the phenotype of

the ‘uncoupling’ mutations like *mom^{th211}*, *boz^{m168}*, *flhⁿ¹* and *ntl^{b160}*.

Left-right asymmetry of the pancreas requires *spaw*

It was of interest to know whether *spaw* function is also required for the asymmetry of other visceral organs. In zebrafish, the embryonic pancreas is normally positioned to the right of the dorsal midline and this is first evident at ~36 hours after fertilization. Defective LR patterning causes the pancreas to be mispositioned to the left-side or to remain in a midline position (Yan et al., 1999). The displacement of the endocrine pancreas can be visualized using an in situ probe for the *preproinsulin* gene (Fig. 5K,L) (Milewski et al., 1998). Inhibition of *spaw* led to an increase in the frequency of misplacement of the pancreas, either to a reversed (left-sided) position or, more frequently, to a midline placement (Table 2C). These results are in agreement with earlier observations that a partial loss of zygotic *oep* activity disrupts pancreatic LR asymmetry (Yan et al., 1999).

Regulation of asymmetrically expressed genes by *spaw*: trunk mesoderm

As *spaw* is required for visceral organ LR asymmetry, one would expect asymmetric gene expression within the left lateral plate mesoderm to be regulated by *spaw*. To test this prediction, we examined the expression of four such left-sided genes, *cyclops*, *lefty1*, *lefty2* and *pix2*, as well as expression of *spaw* itself within the lateral plate. The first four genes initiate asymmetric expression after the onset of left-sided *spaw*

Table 2. Effect of *spaw* knockdown on organ laterality

A Cardiac jogging		Group	n	Heart		
				% L Jog	% R Jog	%No Jog
	NC-MO	28	100	0	0	
	spaw-MO1	27	52	19	30	
	NC-MO	32	78	22	0	
	spaw-MO2	28	36	7	57	
	Uninjected	50	98	2	0	
	Cyc-MO	23	91	9	0	

B Jogging versus looping		Group	n	Jog	% Jog	Heart		
						% D-loop	% L-loop	% No loop
	Uninjected	52	Left jog	100	100	0	0	
			Right jog	0	0	0	0	
			No jog	0	0	0	0	
	NC-MO	57	Left jog	94	98	0	1	
			Right jog	5	0	100	0	
			No jog	0	0	0	0	
	spaw-MO1	55	Left jog	51	56	5	38	
			Right jog	20	50	20	30	
			No jog	28	39	20	40	

C Position of pancreas		Group	n	Pancreas		
				%R	%L	%M
	NC-MO	43	72	7	21	
	spaw-MO1	43	30	21	49	

n, number of embryos; % jog, % of the number of embryos with a left, right or no jog phenotype; % D-loop, the fraction of embryos of a given jogging phenotype that subsequently developed a D-loop. Likewise for % L-loop and % No loop; %R, %L or %M, % of injected embryos with the pancreas positioned to the right or left of the midline or on the midline, respectively; Cyc-MO, *cyclops* morpholino; NC-MO, Gene Tools negative control morpholino; spaw-MO1, *southpaw* morpholino complementary to translation start site; spaw-MO2, *southpaw* morpholino complementary to a splice acceptor site.

The dose of Cyc-MO was 8 ng per embryo. For all other morpholinos, the dose was 10 ng per embryo.

Results shown in B are pooled from two morpholino experiments; results in C are pooled from three morpholino experiments.

Table 3. Effect of *spaw* knockdown on asymmetric gene expression

Gene	Stage for in situ	Morpholino	<i>n</i>	Lateral plate expression (%)				Dorsal diencephalon (%)	
				Left	Right	Bil	Absent	Left	Absent
<i>lefty1</i>	19-22 s	None	44	84	0	0	16	64	34
	19-22 s	NC-MO	29	93	0	0	7	66	34
	19-22 s	<i>spaw</i> -MO1	29	0	0	0	100	3	94
<i>lefty1</i>	21-23 s	None	30	60	0	0	40	80	20
	21-23 s	NC-MO	26	42	4	0	56	81	19
	21-23 s	<i>spaw</i> -MO2	27	7	0	0	93	11	89
<i>cyclops</i>	18-20 s	NC-MO	21	86	5	0	9	67	29
	18-20 s	<i>spaw</i> -MO1	20	5	0	0	95	0	100
<i>cyclops</i>		None	36	14	0	0	86	100	0
	18-22 s	NC-MO	40	20	0	0	80	95	5
	18-22 s	<i>spaw</i> -MO1	40	17	0	0	83	15	85
<i>pitx2</i>	22-24 s	None	42	95	0	0	5	98	2
	22-24 s	NC-MO	32	100	0	0	0	100	0
	22-24 s	<i>spaw</i> -MO1	36	3	0	0	97	6	94
<i>southpaw</i>	16-18 s	None	36	92	0	8	0		
	16-18 s	NC-MO	47	83	2	11	4		
	16-18 s	<i>spaw</i> -MO1	46	22	0	0	78		
<i>southpaw</i>	18-20 s	None	34	100	0	0	0		
	18-20 s	NC-MO	21	95	0	0	5		
	18-20 s	<i>spaw</i> -MO2	19	5	0	0	95		
<i>lefty2</i>	19-23 s	None	42	81	0	0	19		
	19-23 s	NC-MO	38	79	0	0	21		
	19-23 s	<i>spaw</i> -MO1	41	0	0	0	100		

s, somites; *n*, number of embryos injected; %, % of injected embryos with expression of a given marker gene in a given territory; Bil, bilateral. MO dose was 10 ng per embryo.

Lateral plate expression of *pitx2* was evaluated by monitoring changes in left-side *pitx2c* expression near the posterior gut.

expression and therefore are candidates for downstream, Spaw-dependent genes. Asymmetric *spaw* expression was blocked by Spaw-MO1, but the bilateral *spaw* domains near the tailbud were unaffected (Fig. 7A-C). The effect on *spaw* expression itself is not unexpected, as studies in other animals have demonstrated the existence of an autoregulatory loop for a subset of the expression domains of several *nodal*-related genes (reviewed by Hamada et al., 2002; Wright, 2001). Asymmetric mesodermal expression of *cyclops*, *lefty1*, *lefty2* and *pitx2* was lost in 80-100% of Spaw-MO1-injected embryos (Table 3; Fig. 7E-G). *lefty1* expression in the posterior notochord was also consistently lost or reduced (Fig. 7H) (Spaw dependence of *lefty1* in anterior and middle parts of the notochord could not be determined because of the variability of wild-type *lefty1* expression in these regions). A similar dependence of midline (floorplate) *lefty1* expression on late Nodal signaling has been reported previously for some mouse *nodal* alleles (Lowe et al., 2001; Norris et al., 2002). None of these effects was seen when a control MO was injected (Table 3; Fig. 7A,E-H). Spaw-MO2 had similar effects on *lefty1* and *spaw* expression as seen with the translation-inhibiting morpholino Spaw-MO1 (Table 3). As mentioned before, expression of midline markers was not affected at either early or late stages (Fig. 5E, Fig. 6, Fig. 7B-D). Likewise, the *spaw* morpholinos did not perturb bilateral domains of gene expression, as evidenced by normal bilateral expression of *oep* within the lateral plate mesoderm (Fig. 7D), bilateral expression of *oep* and *flh* in the dorsal diencephalon (Fig. 7L-O) and the bilateral expression of *pitx2* in the putative Rohon-Beard cells, the ventral CNS and the hatching gland (Fig. 7E,P-S; data not shown).

Finally, as an additional test of specificity, we checked whether Spaw protein could rescue the effect of Spaw-MO1. Mature Spaw ligand was introduced into Spaw-MO1-injected embryos by co-injection of *ActHASpaw* RNA, which is resistant to the inhibitory effects of the Spaw-MOs. In order to minimize the risk of dorsalization artifacts, we were constrained to using low doses that would, presumably, result in lower rescue efficiencies. Endogenous *spaw* transcripts were distinguished from injected *ActHASpaw* RNA by using a probe specific for sequences corresponding to the Spaw prepro region. In 15-20% of the co-injected embryos, there was enough Spaw activity restored to rescue the *spaw* autoregulatory loop, as indicated by the activation of expression of the endogenous *spaw* gene within the lateral plate at the 16-18 somite stage (Table 4, Fig. 7T-W). Reversal of the asymmetry of *spaw* gene expression in the lateral plate was seen in some injected embryos (Fig. 7V,W); this presumably reflects right-sided enrichment of the rescuing *ActHASpaw* RNA, plus continued inhibition by Spaw-MO1 on the left side. In summary, the LR patterning defects seen with the Spaw-MOs are not caused by a generalized or nonspecific disruption of gene expression within the brain, dorsal midline or LPM, but reflect the specific inhibition of the *spaw* transcripts.

Regulation of asymmetrically expressed genes by *spaw*: the diencephalon

We have never detected *spaw* expression within the CNS (Fig. 2H; data not shown). In light of this, we were very surprised to find that the morpholino-mediated inhibition of *spaw* also

Table 4. Rescue of lateral plate expression by Spaw ligand

Gene	Stage	Injection	n	Lateral plate expression	
				% <i>spaw</i> ⁺	% <i>spaw</i> ⁻
<i>southpaw</i>	16-18 s	None	22	100	0
	16-18 s	<i>spaw</i> -MO1	34	3	97
	16-18 s	<i>spaw</i> -MO1 +ActHAspaw RNA	78	18	82
<i>southpaw</i>	17-19 s	None	65	11	89
	17-19 s	<i>spaw</i> -MO1	45	15	85
	17-19 s	<i>spaw</i> -MO1 +ActHAspaw RNA	38	32	68

s, somites; n, number of embryos injected; % *spaw*⁺, % of injected embryos with expression of the endogenous *spaw* gene in lateral plate, either unilaterally or bilaterally.
Spaw-MO1 dose was 9 ng per embryo; *ActHAspaw* RNA dose was 40 pg per embryo.
 Probe used was DNP-*Spaw* (minus mature region) probe.

had a strong effect on diencephalic LR asymmetry. All early markers of diencephalic LR polarity (*cyclops*, *lefty1*, *pitx2*) were strongly downregulated in *Spaw*-MO1-injected embryos (Table 3; Fig. 7H-K,P-S). Similar results were seen with *Spaw*-MO2 in the case where the comparison was made (Table 3). To some degree, the effect on *lefty1* may be a secondary consequence of the loss of diencephalic *cyclops* expression, as diencephalic *lefty1* (but not *cyclops* or *pitx2*) is strongly reduced in *cyclops* mutants (Liang et al., 2000). For each of these markers, the peak stages of diencephalic and visceral asymmetry are out of phase with each other, and this makes it difficult to simultaneously score the effects on both visceral and diencephalic asymmetry. However, in some experiments, we were able to score both regions simultaneously and found that trunk and neural LR asymmetry were both strongly suppressed in the same batch of *Spaw*-MO1-injected embryos (Table 3). In the brain, the left-sided expression domains of *cyclops*, *lefty1* and *pitx2* lie within the epiphyseal region of the diencephalon (Liang et al., 2000). The *spaw* morpholinos had no effect on genes that are expressed bilaterally within the epiphysis, either at early or late stages of somitogenesis [12-14 somites, *oep* (Fig. 7L,M); 19-23 somites, *flh* (Fig. 7N,O)].

DISCUSSION

Conservation of Nodal function in visceral LR asymmetry in the zebrafish

nodal-related genes show a conserved pattern of asymmetric expression within the left lateral plate mesoderm in mice, chickens and frogs (reviewed by Hamada et al., 2001). The expression pattern of the human *nodal-related* gene(s) is not known, but studies of human EGF-CFC mutations support a role for Nodal proteins in human laterality as well (Bamford et al., 2000). In the zebrafish, the *nodal*-related gene *cyclops* exhibits the same conserved pattern of expression. However, *cyclops* mutations have, at best, only a minor effect on visceral LR asymmetry. This observation raises the issue of whether the function of Nodal signaling in LR patterning is conserved in the zebrafish. Our experiments resolve this by showing that there is another *nodal*-related gene, *spaw*, that is expressed

asymmetrically within the zebrafish lateral plate. Morpholino experiments show that *spaw* is absolutely required for normal visceral LR asymmetry but is not required for development of dorsal midline structures. Thus, *pitx2*, a target of asymmetric Nodal signaling in other vertebrates (reviewed by Yost, 2001), is strongly downregulated or abolished within the left LPM of embryos with reduced *Spaw* activity. *spaw* transcripts were not detected before the start of somitogenesis, and asymmetric *spaw* expression is seen only in the left lateral plate. In light of these observations, we interpret the morpholino defects as reflecting a requirement for Nodal (*Spaw*) signaling within the left lateral plate mesoderm. Our results are consistent with the observations from studies of mouse *nodal* alleles with reduced activity or expression in the left lateral plate (Brennan et al., 2002; Lowe et al., 2001; Norris et al., 2002). Whether asymmetric *cyclops* expression in the LPM contributes in a subtle way to visceral LR asymmetry remains to be determined.

Analyses of the mouse *nodal* and *Xenopus xnr1* promoters have revealed that stable *nodal* gene expression often requires a positive autoregulatory loop. This loop is mediated by cis-acting elements containing Foxh1/Fast-binding sites (Norris and Robertson, 1999; Osada et al., 2000; Saijoh et al., 2000). The phenotype of zebrafish *foxh1/sur* mutations implies a similar mechanism for fish, as *sqt* and *cyclops* expression is initiated but not maintained in *sur*^{-/-} homozygotes (Pogoda et al., 2000; Sirotkin et al., 2000b). Consistent with the existence of a positive feedback loop, we find that stable expression of *spaw* transcripts within the left lateral plate requires *Spaw* activity.

Regulation of Nodal signaling in *Xenopus* and mouse embryos also involves negative feedback, whereby nodal ligands induce the synthesis of their own antagonists, the Lefty1 and Lefty2 proteins (Cheng et al., 2000; Lowe et al., 2001). *lefty1* and *lefty2* are also downregulated in zebrafish embryos with reduced levels of *Oep*, a co-factor for Nodal signaling (Yan et al., 1999). Our experiments provide additional evidence for a negative feedback loop in the zebrafish. Morpholino-mediated knockdown of *spaw* essentially abolishes *lefty2* and *lefty1* expression in the LPM and downregulates *lefty1* expression in the posterior part of the notochord. In summary, many of the salient features of the *nodal-lefty-pitx2* 'cassette' are conserved in the zebrafish in the context of *spaw* expression, regulation and function.

Implications for the lateral transfer of LR asymmetry cues from the organizer

The pattern of *spaw* expression in normal and mutant embryos provides insight into the mechanism by which LR asymmetry cues are relayed from the early organizer (shield) to the lateral plate. Asymmetric *spaw* expression initiates near the tailbud before spreading anteriorly; this occurs well after the completion of gastrulation. This observation suggests that the transfer of laterality cues from the early organizer to the lateral plate is mediated by a cell population within or near the tailbud, whose lineage can be traced back to the early organizer. One group of cells that fulfills this criterion is the dorsal forerunner cells. These cells originate in the part of the dorsal organizer that does not involute during gastrulation. The descendants of the forerunner cells ultimately come to reside near the tailbud in a structure known as Kupffer's

vesicle (KV). The cells lining KV are monociliated (Essner et al., 2002), similar to cells within the mouse node that have been implicated in LR patterning of the mouse LPM (reviewed by Hamada et al., 2002) (Hamada et al., 2002; Nonaka et al., 2002; Supp et al., 1997). The fact that mutations in the *boz*, *sqt*, *ntl* and *flh* genes all cause bilateral expression of *spaw* is at least consistent with a role for the forerunner cells in regulating LR asymmetry. *sqt*, *ntl* and *flh* expression overlap within the forerunner cells, and *boz* mutations lead to a downregulation of *sqt* within the forerunner domain (Feldman et al., 1998; Melby et al., 1997; Rebagliati et al., 1998a; Schulte-Merker et al., 1994; Shimizu et al., 2000; Sirotkin et al., 2000a). Likewise, others have suggested a role for the forerunner cells/KV in LR patterning based both on forerunner expression of the zebrafish ortholog of left-right dynein, an axonemal dynein required for visceral LR asymmetry in the mouse (Supp et al., 1997) and on the aforementioned KV expression of monocilia (Essner et al., 2002); both their embryological and genetic data indicate that dorsal forerunner cells and KV are essential for normal LR development (H. J. Yost, personal communication). However, the forerunners are not the only candidates for the transfer of laterality cues from the dorsal organizer to the tailbud. The YSL nuclei that underlie the early organizer will also shift in a manner that parallels the movement of the forerunner cells. In principle, these YSL nuclei could also relay additional LR cues from the early organizer to the tailbud.

Coordination of visceral and diencephalic LR asymmetry

The Swiss embryologist Von Woellarth made some of the earliest observations of linkage between neural and visceral LR asymmetry. He noted an association between reversal of organ situs and reversal of diencephalic LR asymmetry in amphibians in the wild (Von Woellarth, 1950). Consistent with such a linkage, others have shown that Nodal signaling is required for both visceral and diencephalic LR patterning in the zebrafish. *oep* mutants cannot transduce Nodal signals and fail to express left-side-specific asymmetries within both the head and trunk (Concha et al., 2000; Gamse et al., 2002; Liang et al., 2000). Our experiments identify the Spaw protein as a key Nodal signal that is needed for both diencephalic and visceral organ LR asymmetry in the zebrafish.

How are visceral organ and diencephalic LR asymmetry coordinated during embryogenesis? Our data are consistent with the hypothesis that Spaw signaling from the anterior left lateral plate mesoderm induces diencephalic LR asymmetry, either directly through long-range diffusion or through a signaling relay (Fig. 8). The ultimate effect would then be either activation of a left-sided program or, equivalently, the antagonism of a repressor (Concha et al., 2000), in either case leading to left-sided diencephalic expression of *cyclops*, *pitx2* and *lefty1*. Although this model provides a simple explanation of how visceral and diencephalic LR asymmetry can be coordinated, other models cannot be ruled out. For example, because the asymmetric *spaw* pattern is highly dynamic, we cannot yet exclude the possibility of a more anterior, transient domain of *spaw* expression that cues diencephalic LR asymmetry.

Molecular markers of diencephalic asymmetry have not yet been identified in other animals. However, observations in

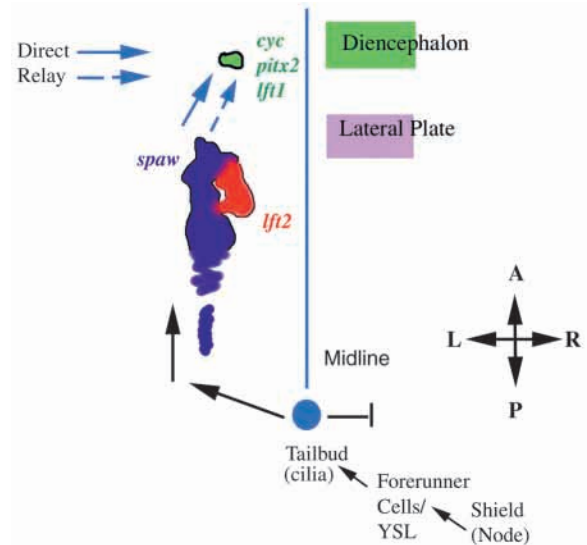


Fig. 8. A model for the coordination of visceral and diencephalic LR asymmetry. LR cues from the dorsal organizer/node (zebrafish shield) are transmitted to the tailbud, possibly by the migration of forerunner cells or YSL nuclei, and these cues activate *spaw* in the left lateral plate (purple). Spaw ligand expressed near the developing heart (red) diffuses to the dorsal diencephalon (unbroken arrow, direct signaling) or initiates an Spaw-dependent relay (broken arrow) that involves other signaling molecules, in order to allow stable *cyclops*, *pitx2c* and *lefty1* expression in the left part of the epiphyseal/habenular region of the diencephalon (green). The blunted line indicates the presence of a midline barrier and/or repression to the right of the zebrafish midline, as implied by several lines of evidence (Chen et al., 1997; Chin et al., 2000; Concha et al., 2000; Danos and Yost, 1996; Liang et al., 2000) (Table 1).

chick embryos suggest that the propagation of asymmetric cues from the trunk to the head might represent a conserved mechanism for coordinating head and visceral LR asymmetry. In stage 9 chick embryos, *cerberus* is expressed in the left lateral plate and in left-side head mesenchyme. *cerberus* expression in the head depends on a chick *nodal*-related gene with a similar spatial pattern. Asymmetric expression of both genes is first seen in the lateral plate. Moreover, implantation of a Nodal pellet in the right flank of chicken embryos induces ectopic *cerberus* expression in the head but does not induce *cerberus* in areas closer to the pellet (Zhu et al., 1999).

Our studies in the zebrafish and those in the chicken suggest that Nodal signaling from the anterior lateral plate may have a critical role in organizing LR asymmetry in the head. One goal of future experiments will be to test directly the hypothesis that *spaw* expression in the anterior lateral plate triggers diencephalic asymmetry.

Note added in proof

Gamse et al. have shown that the left-right placement of the parapineal organ, first evident at 28 hours, subsequently organizes later aspects of diencephalic LR asymmetry in the zebrafish (Gamse et al., 2003). The left-right displacement of the parapineal from the midline may depend on the earlier asymmetric expression of *cyclops*, *pitx2* and *lefty1* within the epiphyseal region.

This work was initiated in the Laboratory of Molecular Genetics-NICHD, NIH. We thank Igor Dawid for supporting the initial stages of this work. Support was provided by a Pilot Award from the University of Iowa Diabetes and Endocrinology Research Center, NIH DK25295 and a Biosciences Pilot Grant from the State of Iowa. We thank Igor Dawid, Diane Slusarski and Rob Cornell for their comments on the manuscript. We also thank Eddy deRobertis, Joe Yost, Donald Steiner, Christine and Bernard Thisse, Sharon Amacher, Jennifer Liang, Marnie Halpern, Rebecca Burdine and Alex Schier for providing reagents and/or useful discussions.

REFERENCES

- Bamford, R. N., Roessler, E., Burdine, R. D., Saplakoglu, U., de la Cruz, J., Splitt, M., Goodship, J. A., Towbin, J., Bowers, P., Ferrero, G. B. et al. (2000). Loss-of-function mutations in the EGF-CFC gene *CFC1* are associated with human left-right laterality defects. *Nat. Genet.* **26**, 365-369.
- Bisgrove, B. W., Essner, J. J. and Yost, H. J. (1999). Regulation of midline development by antagonism of lefty and nodal signaling. *Development* **126**, 3253-3262.
- Bisgrove, B. W., Essner, J. J. and Yost, H. J. (2000). Multiple pathways in the midline regulate concordant brain, heart and gut left-right asymmetry. *Development* **127**, 3567-3579.
- Brennan, J., Norris, D. P. and Robertson, E. J. (2002). Nodal activity in the node governs left-right asymmetry. *Genes Dev.* **16**, 2339-2344.
- Burdine, R. D. and Schier, A. F. (2000). Conserved and divergent mechanisms in left-right axis formation. *Genes Dev.* **14**, 763-776.
- Capdevila, J., Vogan, K. J., Tabin, C. J. and Izpisua Belmonte, J. C. (2000). Mechanisms of left-right determination in vertebrates. *Cell* **101**, 9-21.
- Chen, J. N., van Eeden, F. J., Warren, K. S., Chin, A., Nusslein-Volhard, C., Haffter, P. and Fishman, M. C. (1997). Left-right pattern of cardiac BMP4 may drive asymmetry of the heart in zebrafish. *Development* **124**, 4373-4382.
- Cheng, A. M., Thisse, B., Thisse, C. and Wright, C. V. (2000). The lefty-related factor *Xatv* acts as a feedback inhibitor of nodal signaling in mesoderm induction and L-R axis development in xenopus. *Development* **127**, 1049-1061.
- Chin, A. J., Tsang, M. and Weinberg, E. S. (2000). Heart and gut chiralities are controlled independently from initial heart position in the developing zebrafish. *Dev. Biol.* **227**, 403-421.
- Concha, M. L., Burdine, R. D., Russell, C., Schier, A. F. and Wilson, S. W. (2000). A nodal signaling pathway regulates the laterality of neuroanatomical asymmetries in the zebrafish forebrain. *Neuron* **28**, 399-409.
- Danos, M. C. and Yost, H. J. (1996). Role of notochord in specification of cardiac left-right orientation in zebrafish and *Xenopus*. *Dev. Biol.* **177**, 96-103.
- Essner, J. J., Branford, W. W., Zhang, J. and Yost, H. J. (2000). Mesendoderm and left-right brain, heart and gut development are differentially regulated by *pitx2* isoforms. *Development* **127**, 1081-1093.
- Essner, J. J., Vogan, K. J., Wagner, M. K., Tabin, C. J., Yost, H. J. and Brueckner, M. (2002). Conserved function for embryonic nodal cilia. *Nature* **418**, 37-38.
- Fekany, K., Yamanaka, Y., Leung, T., Sirotkin, H. I., Topczewski, J., Gates, M. A., Hibi, M., Renucci, A., Stemple, D., Radbill, A. et al. (1999). The zebrafish *bozozok* locus encodes Dharma, a homeodomain protein essential for induction of gastrula organizer and dorsoanterior embryonic structures. *Development* **126**, 1427-1438.
- Feldman, B., Gates, M. A., Egan, E. S., Dougan, S. T., Rennebeck, G., Sirotkin, H. I., Schier, A. F. and Talbot, W. S. (1998). Zebrafish organizer development and germ-layer formation require nodal-related signals. *Nature* **395**, 181-185.
- Game, J. T., Shen, Y. C., Thisse, C., Thisse, B., Raymond, P. A., Halpern, M. E. and Liang, J. O. (2002). *Otx5* regulates genes that show circadian expression in the zebrafish pineal complex. *Nat. Genet.* **30**, 117-121.
- Game, J. T., Thisse, C., Thisse, B. and Halpern, M. E. (2003). The parapineal mediates left-right asymmetry in the zebrafish diencephalon. *Development* **130**, 1059-1068.
- Griffin, K. J., Amacher, S. L., Kimmel, C. B. and Kimelman, D. (1998). Molecular identification of *spadetail*: regulation of zebrafish trunk and tail mesoderm formation by T-box genes. *Development* **125**, 3379-3388.
- Gritsman, K., Zhang, J., Cheng, S., Heckscher, E., Talbot, W. S. and Schier, A. F. (1999). The EGF-CFC protein one-eyed pinhead is essential for nodal signaling. *Cell* **97**, 121-132.
- Hamada, H., Meno, C., Saijoh, Y., Adachi, H., Yashiro, K., Sakuma, R. and Shiratori, H. (2001). Role of asymmetric signals in left-right patterning in the mouse. *Am. J. Med. Genet.* **101**, 324-327.
- Hamada, H., Meno, C., Watanabe, D. and Saijoh, Y. (2002). Establishment of vertebrate left-right asymmetry. *Nat. Rev. Genet.* **3**, 103-113.
- Ho, C. Y., Houart, C., Wilson, S. W. and Stainier, D. Y. (1999). A role for the extraembryonic yolk syncytial layer in patterning the zebrafish embryo suggested by properties of the *hex* gene. *Curr. Biol.* **9**, 1131-1134.
- Jones, C. M., Kuehn, M. R., Hogan, B. L., Smith, J. C. and Wright, C. V. (1995). Nodal-related signals induce axial mesoderm and dorsalize mesoderm during gastrulation. *Development* **121**, 3651-3662.
- Karlen, S. and Rebagliati, M. (2001). A morpholino phenocopy of the cyclops mutation. *Genesis* **30**, 126-128.
- Kudoh, T., Tsang, M., Hukriede, N. A., Chen, X., Dedekian, M., Clarke, C. J., Kiang, A., Schultz, S., Epstein, J. A., Toyama, R. et al. (2001). A gene expression screen in zebrafish embryogenesis. *Genome Res.* **11**, 1979-1987.
- Liang, J. O., Etheridge, A., Hantsoo, L., Rubinstein, A. L., Nowak, S. J., Izpisua Belmonte, J. C. and Halpern, M. E. (2000). Asymmetric nodal signaling in the zebrafish diencephalon positions the pineal organ. *Development* **127**, 5101-5112.
- Liao, W., Ho, C. Y., Yan, Y. L., Postlethwait, J. and Stainier, D. Y. (2000). Hhex and scl function in parallel to regulate early endothelial and blood differentiation in zebrafish. *Development* **127**, 4303-4313.
- Long, S. and Rebagliati, M. (2002). Sensitive two-color whole-mount in situ hybridizations using digoxigenin- and dinitrophenol-labeled RNA probes. *Biotechniques* **32**, 494, 496, 498.
- Lowe, L. A., Supp, D. M., Sampath, K., Yokoyama, T., Wright, C. V., Potter, S. S., Overbeek, P. and Kuehn, M. R. (1996). Conserved left-right asymmetry of nodal expression and alterations in murine situs inversus. *Nature* **381**, 158-161.
- Lowe, L. A., Yamada, S. and Kuehn, M. R. (2001). Genetic dissection of nodal function in patterning the mouse embryo. *Development* **128**, 1831-1843.
- Melby, A. E., Kimelman, D. and Kimmel, C. B. (1997). Spatial regulation of floating head expression in the developing notochord. *Dev. Dyn.* **209**, 156-165.
- Milewski, W. M., Duguay, S. J., Chan, S. J. and Steiner, D. F. (1998). Conservation of PDX-1 structure, function, and expression in zebrafish. *Endocrinology* **139**, 1440-1449.
- Nonaka, S., Shiratori, H., Saijoh, Y. and Hamada, H. (2002). Determination of left-right patterning of the mouse embryo by artificial nodal flow. *Nature* **418**, 96-99.
- Norris, D. P. and Robertson, E. J. (1999). Asymmetric and node-specific nodal expression patterns are controlled by two distinct cis-acting regulatory elements. *Genes Dev.* **13**, 1575-1588.
- Norris, D. P., Brennan, J., Bikoff, E. K. and Robertson, E. J. (2002). The *Foxh1*-dependent autoregulatory enhancer controls the level of Nodal signals in the mouse embryo. *Development* **129**, 3455-3468.
- Osada, S. I., Saijoh, Y., Frisch, A., Yeo, C. Y., Adachi, H., Watanabe, M., Whitman, M., Hamada, H. and Wright, C. V. (2000). Activin/nodal responsiveness and asymmetric expression of a *Xenopus* nodal-related gene converge on a FAST-regulated module in intron 1. *Development* **127**, 2503-2514.
- Piccolo, S., Agius, E., Leyns, L., Bhattacharyya, S., Grunz, H., Bouwmeester, T. and de Robertis, E. M. (1999). The head inducer Cerberus is a multifunctional antagonist of Nodal, BMP and Wnt signals. *Nature* **397**, 707-710.
- Pogoda, H. M., Solnica-Krezel, L., Driever, W. and Meyer, D. (2000). The zebrafish forkhead transcription factor *FoxH1/Fast1* is a modulator of nodal signaling required for organizer formation. *Curr. Biol.* **10**, 1041-1049.
- Rebagliati, M. R., Toyama, R., Fricke, C., Haffter, P. and Dawid, I. B. (1998a). Zebrafish nodal-related genes are implicated in axial patterning and establishing left-right asymmetry. *Dev. Biol.* **199**, 261-272.
- Rebagliati, M. R., Toyama, R., Haffter, P. and Dawid, I. B. (1998b). *cyclops* encodes a nodal-related factor involved in midline signaling. *Proc. Natl. Acad. Sci. USA* **95**, 9932-9937.
- Saijoh, Y., Adachi, H., Sakuma, R., Yeo, C. Y., Yashiro, K., Watanabe, M., Hashiguchi, H., Mochida, K., Ohishi, S., Kawabata, M. et al. (2000).

- Left-right asymmetric expression of *lefty2* and *nodal* is induced by a signaling pathway that includes the transcription factor FAST2. *Mol. Cell* **5**, 35-47.
- Sampath, K., Rubinstein, A. L., Cheng, A. M., Liang, J. O., Fekany, K., Solnica-Krezel, L., Korzh, V., Halpern, M. E. and Wright, C. V.** (1998). Induction of the zebrafish ventral brain and floorplate requires cyclops/nodal signalling. *Nature* **395**, 185-189.
- Schulte-Merker, S., van Eeden, F. J., Halpern, M. E., Kimmel, C. B. and Nusslein-Volhard, C.** (1994). *no tail (ntl)* is the zebrafish homologue of the mouse *T (Brachyury)* gene. *Development* **120**, 1009-1015.
- Shimizu, T., Yamanaka, Y., Ryu, S. L., Hashimoto, H., Yabe, T., Hirata, T., Bae, Y. K., Hibi, M. and Hirano, T.** (2000). Cooperative roles of *Bozozok/Dharma* and *Nodal*-related proteins in the formation of the dorsal organizer in zebrafish. *Mech. Dev.* **91**, 293-303.
- Sirotkin, H. I., Dougan, S. T., Schier, A. F. and Talbot, W. S.** (2000a). *bozozok* and *squint* act in parallel to specify dorsal mesoderm and anterior neuroectoderm in zebrafish. *Development* **127**, 2583-2592.
- Sirotkin, H. I., Gates, M. A., Kelly, P. D., Schier, A. F. and Talbot, W. S.** (2000b). *Fast1* is required for the development of dorsal axial structures in zebrafish. *Curr. Biol.* **10**, 1051-1054.
- Supp, D. M., Witte, D. P., Potter, S. S. and Brueckner, M.** (1997). Mutation of an axonemal dynein affects left-right asymmetry in *inversus viscerum* mice. *Nature* **389**, 963-966.
- Tsang, M., Kim, R., de Caestecker, M. P., Kudoh, T., Roberts, A. B. and Dawid, I. B.** (2000). Zebrafish *nma* is involved in TGFbeta family signaling. *Genesis* **28**, 47-57.
- Von Woellwarth, C.** (1950). Experimentelle Untersuchungen über den Situs Inversus der Eingeweide und der Habenula des Zwischenhirns bei Amphibien. *Roux Arch. Entw. Mech. Organ.* **144**, 178-256.
- Wallace, K. N., Yusuff, S., Sonntag, J. M., Chin, A. J. and Pack, M.** (2001). Zebrafish *hhex* regulates liver development and digestive organ chirality. *Genesis* **30**, 141-143.
- Wright, C. V.** (2001). Mechanisms of left-right asymmetry: what's right and what's left? *Dev. Cell* **1**, 179-186.
- Yan, Y. T., Gritsman, K., Ding, J., Burdine, R. D., Corrales, J. D., Price, S. M., Talbot, W. S., Schier, A. F. and Shen, M. M.** (1999). Conserved requirement for EGF-CFC genes in vertebrate left-right axis formation. *Genes Dev.* **13**, 2527-2537.
- Yost, H. J.** (2001). Establishment of left-right asymmetry. *Int. Rev. Cytol.* **203**, 357-381.
- Zhou, X., Sasaki, H., Lowe, L., Hogan, B. L. and Kuehn, M. R.** (1993). *Nodal* is a novel TGF-beta-like gene expressed in the mouse node during gastrulation. *Nature* **361**, 543-547.
- Zhu, L., Marvin, M. J., Gardiner, A., Lassar, A. B., Mercola, M., Stern, C. D. and Levin, M.** (1999). *Cerberus* regulates left-right asymmetry of the embryonic head and heart. *Curr. Biol.* **9**, 931-938.